Infrared Spectroscopy Study of Microstructures of Poly(silsesquioxane)s

E. S. Park,[†] H. W. Ro,[†] C. V. Nguyen,[‡] R. L. Jaffe,[§] and D. Y. Yoon*,[†]

Department of Chemistry, Seoul National University, Seoul, 151-747, Korea, ELORET Corporation, NASA Ames Research Center, MS 229-1, Moffett Field, California 94305, and NASA Ames Research Center, MS 230-1, Moffett Field, California 94305

Received June 12, 2007. Revised Manuscript Received November 2, 2007

Results are presented from theoretical and experimental infrared (IR) spectroscopy studies of the microstructures of poly(silsesquioxane)s (PSSQs) of varying chemical composition. The calculated IR spectra show two distinct asymmetric Si−O−Si stretch vibration bands for models of complete polyhedral cages, incomplete open cages, and short ladder structures. Close analyses of the calculated results indicate that the higher frequency IR band at about 1150 cm^{-1} is derived from the parallel asymmetric Si−O−Si stretch vibration mode in the $(Si-O)_n$ ring subunit while the lower frequency band at about 1050 cm^{-1} is due to the asymmetric Si−O−Si stretch symmetric with respect to the inversion point at the center of the $(Si-O)_n$ ring and is absent in highly symmetric cage structures. Experimentally, poly(methylsilsesquioxane) (PMSQ), poly(isobutylsilsesquioxane) (PiBSQ), and poly(phenylsilsesquioxane) (PPhSQ) exhibit a varying tendency of cage-like structures, rather than ladder structures, in as-polymerized samples. When the thermal conversion (curing) temperature is increased to 400 °C, the microstructure of PMSQ in thin solid films transforms from open cage-like structure toward a random network with lower symmetry. This change in microstructure is caused by the secondary condensation reaction and the evaporation of cage structures, and the effect of cage evaporation becomes most pronounced for PiBSQ films, which are mostly comprised of cage-like structures that evaporate around 280 °C. In comparison, PPhSQ films retain cage-like structure upon curing to 400 °C as a result of the high evaporation temperature (ca. 500 °C) of the cages.

Introduction

Poly(silsesquioxane)s (PSSQs) are organosilicates with an empirical formula $(RSiO_{1.5})_n$, where R can be hydrogen, methyl, phenyl, or higher molecular weight organic groups. PSSQs were developed over 60 years ago and have found many applications. For example, PSSQ is the first silicone commercialized for application as a high temperature electrical insulation material.[1] In recent years, poly(hydridosilsesquioxane) (PHSQ with R = H) and poly(methylsilsesquioxane) (PMSQ with R = CH_3) have emerged as low dielectric constant interlayer materials for interconnects in microelectronic devices because of their excellent thermal and electrical properties.[2–6] Films of SiO_x containing methyl substituents, which resemble PMSQ and are called organosilicate glasses (OSGs), have been generated by a chemical vapor deposition (CVD) technique and are currently applied as the interlayer dielectric material in the most advanced semiconductor devices with a 65 nm critical dimension. It has been shown that the dielectric constants of these materials are directly related to the degree of methylation, decreasing from 4.1 for SiO_x down to 2.7 as the degree of methylation is increased to 25%.[7]

Nanoporous PMSQs and OSGs with even lower dielectric constants have also been prepared, demonstrating the possibility of further extending the application of this material to future generations of nanoscale semiconductors with feature sizes smaller than 50 nm.[8–10] The porous PMSQ film is prepared by incorporating an organic pore generation material (porogen) into a PMSQ matrix. During the thermal conversion (curing) of the as-polymerized soluble polymer at high temperatures to 400 °C, the porogen is thermally decomposed and volatilized leaving behind stable nanoscale pores. PMSQ films with 30% porosity have been prepared and found to have a dielectric constant as low as 2. Recently, nanoimprint patterning of PSSQs, also called organosilicate polymers, has become of significant interest because of the

* Corresponding author. Phone: +82-2-880-6648. Fax: +82-2-877-6814. E-mail: dyyoon@snu.ac.kr.
[†] Seoul National University.
[‡] ELORET Corporation.
[§] NASA Ames Research Center.

(1) Baney, R. H.; Itoh, M.; Sakakibara, A.; Suzuki, T. *Chem. Rev.* **1995**, *95*, 1409.
(2) Miller, R. D. *Science* **1999**, *286*, 421.
(3) Mikoshiba, S.; Hayase, S. *J. Mater. Chem.* **1999**, *9*, 591.
(4) Wang, C. Y.; Zheng, J. Z.; Shen, Z. X.; Lin, Y.; Wee, A. T. S. *Thin Solid Films* **2001**, *397*, 90.
(5) Lazzeri, P.; Rubloff, G. W.; Vanzetti, L.; Briber, R. M.; Anderle, M.; Bersani, M.; Park, J. J.; Kim, H.-C.; Volksen, W.; Miller, R. D.; Lin, Z. *Surf. Interface Anal.* **2004**, *36*, 304.
(6) Liu, W.-C.; Yu, Y.-Y.; Chen, W.-C. *J. Appl. Polym. Sci.* **2004**, *91*, 2653.
(7) Peters, L. *Semicond. Int.* **1998**, 64.
(8) Nguyen, C. V.; Carter, K. R.; Hawker, C. J.; Hedrick, J. L.; Jaffe, R. L.; Miller, R. D.; Remenar, J. F.; Rhee, H.-W.; Rice, P. M.; Toney, M. F.; Trollsas, M.; Yoon, D. Y. *Chem. Mater.* **1999**, *11*, 3080.
(9) Huang, Q. R.; Volksen, W.; Huang, E.; Toney, M.; Frank, C. W.; Miller, R. D. *Chem. Mater.* **2002**, *14*, 3676.
(10) Grill, A. In *Dielectric Films for Advanced Microelectronics*; Baklanov, M., Green, M., Maex, K., Eds.; Wiley: New York, 2007; p 1.

10.1021/cm071575z CCC: $40.75
Published on Web 01/16/2008

simplification of multilevel interconnect fabrication by the nanoimprint lithography employing solution-processed dielectric materials.[11] In addition, porous PSSQs are also of significant interest for optical wave guides,[12] separations and membranes,[13] catalyst supports,[14] and biotechnology applications.[15]

Despite the importance of PSSQs for a variety of applications, their microstructure at the molecular level is not well understood. Specifically, it is difficult to determine whether the PSSQ molecules are comprised of closed cages, partially open cages, (double chain) ladders, or random network structures. The ability to obtain such information from a simple infrared (IR) spectroscopic technique will be very important for understanding the structure–property relationships of PSSQs and for improving the desired physical properties by modifying the monomer structures[16] and incorporating co-monomers.[17] In this regard, the most relevant IR absorption band is the asymmetrical Si−O−Si stretching mode in the 1000–1200 cm^{-1} region which is likely to be little affected by the nature of the substituent R.[18] Therefore, the analysis of the Si−O−Si stretching vibration modes has commonly been employed for characterizing various PSSQ and OSG films since the early work by Brown et al.[19,20]The IR absorption characteristics of oligomeric cage-containing compounds are quite simple and clearly established.[20–23] However, PSSQ and OSG samples normally exhibit complicated IR absorption features, and their analyses in terms of (double chain) ladder structures[19,20,24,25] or cage/network mixtures,[26,27] for example, have been very ambiguous and confusing.

In this paper, we report the predicted IR frequencies for various microstructure models of PSSQs obtained from high-level ab initio quantum chemistry calculations and compare the calculated spectra with experiments. Moreover, based on the calculated IR spectra, we elucidate the microstructures of PSSQs with various organic substituents of methyl, isobutyl, and phenyl group as a function of the thermal conversion (curing) temperature.

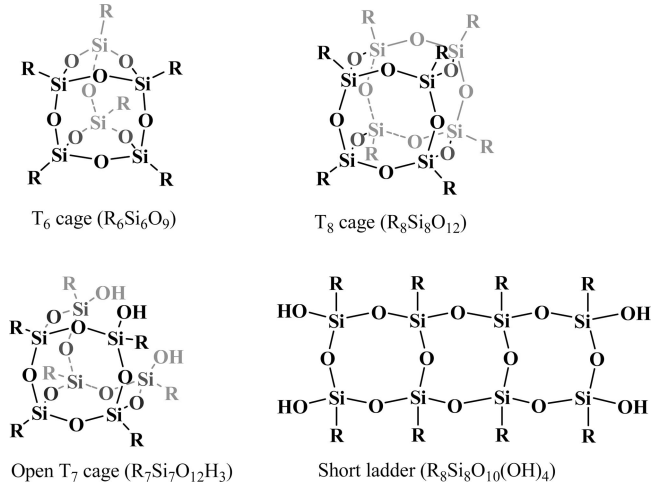

Figure 1. Structure examples of a T_6 cage ($R_6Si_6O_9$), a T_8 cage ($R_8Si_8O_{12}$), an open T_7 cage ($R_7Si_7O_{12}H_3$), and a short ladder ($R_8Si_8O_{10}(OH)_4$).

Computational Method

The geometries, relative energies, and IR spectra of model HSQ and MSQ molecules were obtained from quantum chemistry calculations using the Gaussian98 computer program.[28] The calculations were carried out using the density functional theory (DFT) with the hybrid B3LYP functional and the 6-31G(d) atomic orbital basis set. The IR spectra were generated from the calculated harmonic frequencies and fundamental intensities by assuming a Gaussian line shape with a half-width of 10 cm^{-1} for each vibrational mode. The model molecules considered include cages with 4–12 Si atoms (denoted T_n where n is the number of Si atoms with molecular formula $R_nSi_nO_{1.5n}$), a partially open T_7 cage $R_7Si_7O_{12}H_3$ (the T_8 cage with one Si−R removed and the three dangling Si−O bonds terminated with hydrogens), and short ladder structures such as $R_8Si_8O_{10}(OH)_4$ consisting of three fused Si_4O_4 rings with OH groups to tie off the dangling Si bonds as shown in Figure 1. The cage structures can be thought of as polyhedra with Si atoms at the vertices and O atoms at the midpoints of the edges. The polyhedra considered are tetrahedron, triangular prism, cube, and pentagonal prism for T_4, T_6, T_8, and T_{10}, respectively. For T_{12} both a hexagonal prism and a polyhedron consisting of four pentagonal and four square faces with D_{2d} symmetry were considered.

Experimental Section

Samples. Low molecular weight samples of PMSQ, poly(isobutylsilsesquioxane) (PiBSQ), and poly(phenylsilsesquioxane)

(11) Stewart, M. D.; Willson, C. G. *MRS Bull.* **2005**, *30*, 947.
(12) Scott, B. J.; Wirnsberger, G.; Stucky, G. D. *Chem. Mater.* **2001**, *13*, 3140.
(13) Yang, P.; Wirnsberger, G.; Huang, H. C.; Cordero, S. R.; McGehee, M. D.; Scott, B.; Deng, T.; Whitesides, G. M.; Chmelka, B. F.; Buratto, S. K.; Stucky, G. D. *Science* **2000**, *287*, 465.
(14) Dong, H.; Brook, M. A.; Brennan, J. D. *Chem. Mater.* **2005**, *17*, 2807.
(15) Kim, H.-C.; Kreller, C. R.; Tran, K. A.; Sisodiya, V.; Angelos, S.; Wallraff, G.; Swanson, S.; Miller, R. D. *Chem. Mater.* **2004**, *16*, 4267.
(16) Kim, H.-J.; Lee, J.-K.; Kim, J.-B.; Park, E. S.; Park, S.-J.; Yoo, D. Y.; Yoon, D. Y. *J. Am. Chem. Soc.* **2001**, *123*, 12121.
(17) Ro, H. W.; Char, K.; Jeon, E.-C.; Kim, H.-J.; Kwon, D.; Lee, H.-J.; Lee, J.-K.; Rhee, H.-W.; Soles, C. L.; Yoon, D. Y. *Adv. Mater.* **2007**, *19*, 705.
(18) Brown, J. F, Jr. *J. Am. Chem. Soc.* **1965**, *87*, 4317.
(19) Brown, J. F., Jr *J. Polym. Sci., Part C* **1963**, *1*, 83.
(20) Brown, J. F., Jr.; Vogt, L. H., Jr.; Prescott, P. I. *J. Am. Chem. Soc.* **1964**, *86*, 1120.
(21) Bartsch, M.; Bornhauser, P.; Calzaferri, G.; Imhof, R. *J. Phys. Chem.* **1994**, *98*, 2817.
(22) Marcolli, C.; Calzaferri, G. *J. Phys. Chem. B* **1997**, *101*, 4925.
(23) Kim, S. G.; Choi, J.; Tamaki, R.; Laine, R. M. *Polymer* **2005**, *46*, 4514.
(24) Adachi, H.; Adachi, E.; Hayashi, O.; Okahashi, K. *Rep. Prog. Polym. Phys. Jpn.* **1985**, *28*, 261.
(25) Xie, Z.; He, Z.; Dai, D.; Zhang, R. *Chin. J. Polym. Sci.* **1989**, *7*, 183.
(26) Lee, L.-H.; Chen, W.-C.; Liu, W.-C. *J. Polym. Sci., Part A: Polym. Chem.* **2002**, *40*, 1560.
(27) Grill, A.; Neumayer, D. A. *J. Appl. Phys.* **2003**, *94*, 6697.
(28) Frisch, M. J.; Trucks, G. W.; Schlegel, H. B.; Scuseria, G. E.; Robb, M. A.; Cheeseman, J. R.; Zakrzewski, V. G.; Montgomery, J. A., Jr.; Stratmann, R. E.; Burant, J. C.; Dapprich, S.; Millam, J. M.; Daniels, A. D.; Kuden, K. N.; Strain, M. C.; Farkas, O.; Tomas, J.; Barone, V.; Cossi, M.; Cammi, R.; Menucci, B.; Pomelli, C.; Adamo, C.; Clifford, S.; Ochterski, J.; Petersson, G. A.; Ayala, P. Y.; Cui, Q.; Morokuma, K.; Malick, D. K.; Rabuck, A. D.; Raghavachari, K.; Foresman, J. B.; Cioslowski, J.; Ortiz, J. V.; Stefanov, B. B.; Liu, G.; Liashenko, A.; Piskorz, G.; Kormaromi, I.; Gomperts, R.; Martin, R. L.; Fox, D. J.; Keith, T.; Al-Laham, M. A.; Peng, C. Y.; Nanayakkara, A.; Gonzalez, C.; Challacombe, M.; Gill, P. M. W.; Johnson, B. G.; Chen, W.; Wong, M. W.; Andres, J. L.; Head-Gordon, M.; Replogle, E. S.; Pople, J. A. *GAUSSIAN 98*, Revision A.7; Gaussian Inc.: Pittsburgh, PA, 1998.

Table 1. Vibration Frequencies of PHSQ (R = H) and PMSQ (R = CH_3) Calculated (DFT) and Experimentally Measured (Expt) in cm^{-1}

	T_8 cage (DFT)	T_8 cage (Expt[a])	T_7 open cage (DFT)	PSSQ (Expt[b])
		R = H		
Si−O−Si (ring-asym)	1155	1140	1155	
Si−O−Si (ring-sym)	(1117)	(1117[c])	1119	
Si−H (stretch)	2375	2277	2367–2383	
Si−H (wag)	898	881	867	
O−Si−O (bend)	559	531	597	
Si−O−Si (bend)	451–453	465	450	
		R = CH_3		
Si−O−Si (ring-asym)	1138	1117	1137–1141	1118
Si−O−Si (ring-sym)	(1107)		1101	1037
Si−C (stretch)	1345–1347	1270	1345–1347	1273
Si−C (wag)	856	824	861	856
Si−C (wag)	781	773	776	780, 767
O−Si−O (bend)	510–512	518	514	
Si−O−Si (bend)	450	464	440	

[a] HSQ data are from ref 21, and MSQ data are obtained for the sample obtained from Aldrich Co. [b] The results for PMSQ are taken from Figure 6 (120 °C). [c] Observed in Raman spectra; values in parentheses have negligible IR intensity.

(PPhSQ) were synthesized by the sol–gel method under acidic condition, according to the procedure described previously.[16,17,29,30] The concentration, the molar ratio of catalyst/reactant (r_1), and the molar ratio of water/reactant (r_2) were varied to obtain optimal coating solutions.[29] The spin-coated films of PSSQs were prepared as follows. For PMSQ and PPhSQ, a solution containing 25% (w/w) of the polymers in propylene glycol methyl ether acetate was loaded into a disposable syringe and passed through a 0.2 μm Acrodisc CR PTFE filter directly onto a silicon wafer for IR measurement. The wafer was spun at 2500 rpm for 30 s in the ambient and placed directly into a vacuum furnace. The sample temperature was ramped to and held at the desired temperature for 1 h before cooling, and the final film thickness was about 500 nm. However, in the case of PiBSQ, the Fourier transform infrared (FT-IR) spectra were measured with cured powder samples in a KBr pellet because the thin films of PiBSQ on the silicon wafer did not maintain a good film surface after the thermal curing process (see below). The T_8 cage MSQ powder sample was used as received from Aldrich Co. to prepare the KBr pellet.

Measurements. IR spectra were obtained using a JASCO FT-IR spectrometer (model 660 Plus) at a resolution of 4 cm^{-1} and taking 90 scans per spectrum. Thermogravimetric analysis (TGA, Q50, TA Instrument) was employed for the measurement of weight change as the sample was heated at 10 °C/min. Graphite plate laser desorption/ionization time-of-flight mass spectrometry (GPLDI-TOF MS) of selected PiBSQ sample was carried out as described previously.[16]

Results And Discussion

For the polyhedral cages of HSQ, our calculated relative energies per Si atom are similar to the Hartree–Fock results of Earley[31] and the numerical local density approximation (LDA) results of Ziang et al.[32] in that the T_{10} and T_{12} (D_{2d}) cages are slightly more stable than the T_8 cage and the T_4 and T_6 cages are considerably less stable. The calculated fundamental vibration frequencies, without scaling, for the T_8 HSQ cage are in excellent agreement with the published experimental IR spectrum,[21] as listed in Table 1. The largest error in the theoretical frequency is 4% (98 cm^{-1}) for the Si−H mode, and the corresponding error for the important Si−O−Si stretching modes is 2% (14–20 cm^{-1}).

We compared the theoretical IR spectra for the cage, open cage, and short ladder structures of the HSQ and MSQ model compounds and used the theoretical results for the assignments of the various vibration modes of the PSSQ samples. In particular, we have focused on the Si−O−Si stretching absorption bands in the 1000–1200 cm^{-1} region. The calculated IR spectra of the model compounds of HSQ T_6 cage and Si_8 ladder structures (Figure 2a,b) feature two bands derived from displacements of the O atoms relative to Si in the $(SiO)_n$ rings at around 1050 cm^{-1} and 1150 cm^{-1}, respectively. For each Si−O−Si ring edge, these modes are all classified as asymmetric Si−O−Si stretch. However, they can combine into symmetric or asymmetric modes with respect to the inversion through the center of the ring. If the O atom displacements on opposite sides of a ring are parallel, as shown schematically in Figure 3a, the mode exhibits a higher frequency around 1150 cm^{-1} (this mode will be referred to as $\nu_{\text{ring-asym}}$). If the O atom displacements on opposite sides of a ring are antiparallel, as shown schematically in Figure 3b, the mode exhibits a lower frequency around 1050–1100 cm^{-1} (this mode will be referred to as $\nu_{\text{ring-sym}}$). It is important to note that the atomic displacements associated with the lower frequency mode are symmetric with respect to the center point of the $(Si-O)_n$ ring; thus, the mode is IR forbidden for cages with $(Si-O)_{2n}$ ring subunits (see Figure 3b). In contrast, for cages with $(Si-O)_{2n+1}$ ring subunits, open cages, and short ladder structures, this symmetry restriction does not apply; hence, this absorption feature is observed in the IR. The higher frequency mode is IR active for all structures containing $(Si-O)_{2n}$ rings.

Calculated IR spectra for more symmetrical polyhedral cage compounds, namely, the Si_8 cage (T_8) structure of HSQ and MSQ, are shown in Figure 4a,b, with the major absorption frequencies listed in Table 1. The Si−H bands in the HSQ spectrum, at about 2390 cm^{-1} and 900 cm^{-1}, assigned as the Si−H stretching and wagging modes, show little change from those of the model HSQ compounds for the Si_6 cage and Si_8 ladder structures. The spectrum for the

(29) Lee, J.-K.; Char, K.; Rhee, H.-W.; Ro, H. W.; Yoo, D. Y.; Yoon, D. Y. *Polymer* **2001**, *42*, 9085.
(30) Park, E. S.; Park, S.-J.; Kim, H.-J.; Lee, J.-K.; Ro, H. W.; Yoon, S.-Y.; Yoon, D. Y. *Polym. Prepr. (Am. Chem. Soc., Div. Polym. Chem.)* **2001**, *42* (2), 891.
(31) Earley, C. W. *J. Phys. Chem.* **1994**, *98*, 8693.
(32) Ziang, K.-H.; Pandey, R.; Pernisz, U. C.; Freeman, C. *J. Phys. Chem. B* **1998**, *102*, 8704.

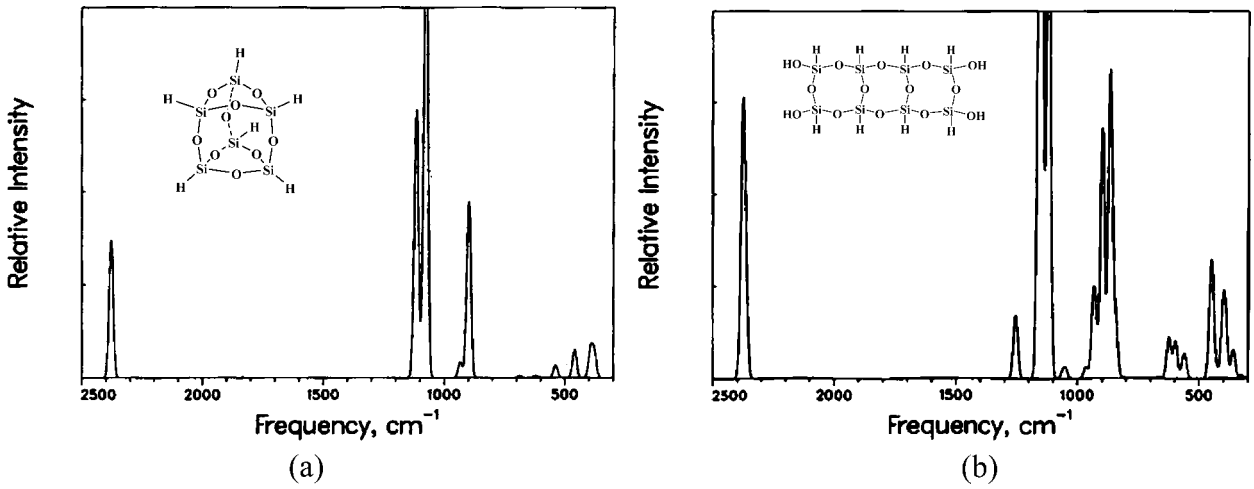

Figure 2. Calculated IR spectra of model compounds of (a) HSQ T_6 cage ($H_6Si_6O_9$) and (b) HSQ Si_8 ladder structure ($R_8Si_8O_{10}(OH)_4$ with R = H).

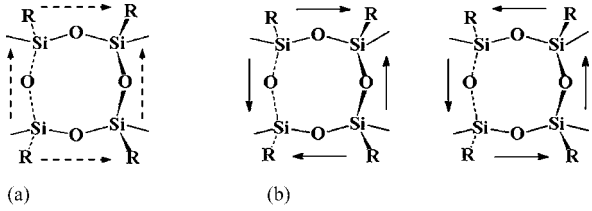

Figure 3. (a) $\nu_{ring\text{-}asym}$ mode and (b) $\nu_{ring\text{-}sym}$ modes of $(Si-O)_4$ ring subunits. The $\nu_{ring\text{-}asym}$ has a high intensity absorption band at about 1150 cm^{-1}, whereas the $\nu_{ring\text{-}sym}$ modes have an absorption band in the range 1050−1115 cm^{-1}.

T_8 MSQ exhibits absorption bands associated with the $Si-CH_3$ stretching mode at about 1340 cm^{-1}. In addition, the T_8 cage MSQ spectrum also contains other $Si-CH_3$ bands, at about 780 cm^{-1} and 860 cm^{-1}, associated with wagging modes. Moreover, these theoretically derived spectra for the T_8 HSQ and MSQ match those of the experimental IR spectra (insets in Figure 4a,b). For the Si−O−Si stretching bands in the two highly symmetrical T_8 HSQ and MSQ structures, it is important to note that the IR spectra exhibit the higher energy $\nu_{ring\text{-}asym}$ band at about 1150 cm^{-1}, whereas the lower energy $\nu_{ring\text{-}sym}$ band is not detected. Consistent with the assignment for the symmetrical $\nu_{ring\text{-}sym}$ stretching bands, it is expected that this band will not be present due to the cancellation of the dipole moments in the highly symmetrical cubic T_8 structure. In contrast, the parallel $\nu_{ring\text{-}asym}$ stretching would exhibit a high absorption intensity as a result of the six $(Si-O)_4$ ring subunits associated with this cubic structure.

Model compounds with opened T_7 cages of HSQ and MSQ are also calculated to further verify the assignment of the vibration modes associated with Si−O bonding. Suffice it to say that these two open cage structures have lower symmetry than the cubic T_8structure and contain fewer $(Si-O)_4$ ring subunits; therefore, it is expected that the IR spectra should contain both Si−O−Si stretching bands. Indeed, the calculated IR spectra (see Figure 5a,b and Table 1) do exhibit both $\nu_{ring\text{-}asym}$ and $\nu_{ring\text{-}sym}$ absorption bands. Furthermore, the Si_6 ladder structure ($R_6Si_6O_7(OH)_4$ with R = CH_3, Figure 5c), which has lower symmetry than the opened cage, shows that the intensity of the 1150 cm^{-1} band is weaker as compared with that of the open cage, while the intensity of the 1050 cm^{-1} band is increased. The results presented here demonstrate that the microstructure of PSSQs can be elucidated to a large degree by IR spectroscopy. In brief, the presence of the $\nu_{ring\text{-}asym}$ band indicates a highly symmetrical structure with $(Si-O)_4$ ring subunits which are found in closed cages and partially open cage structures. The relative intensity of the $\nu_{ring\text{-}sym}$ absorption around 1050 cm^{-1} reflects the local symmetry around the Si−O−Si unit, with the higher intensity indicating a less symmetric, random network structure.

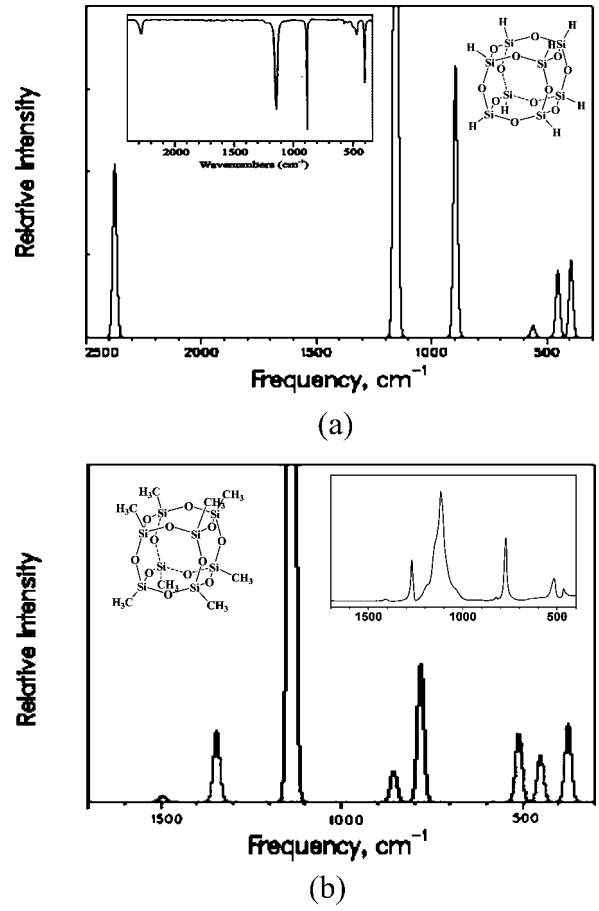

Figure 4. Calculated IR spectra of (a) T_8 of HSQ ($H_8Si_8O_{12}$) (the inset shows experimental data from ref 21) and (b) T_8 of MSQ ($(CH_3)_8Si_8O_{12}$) (the inset shows experimental data obtained for the sample purchased from Aldrich Co.).

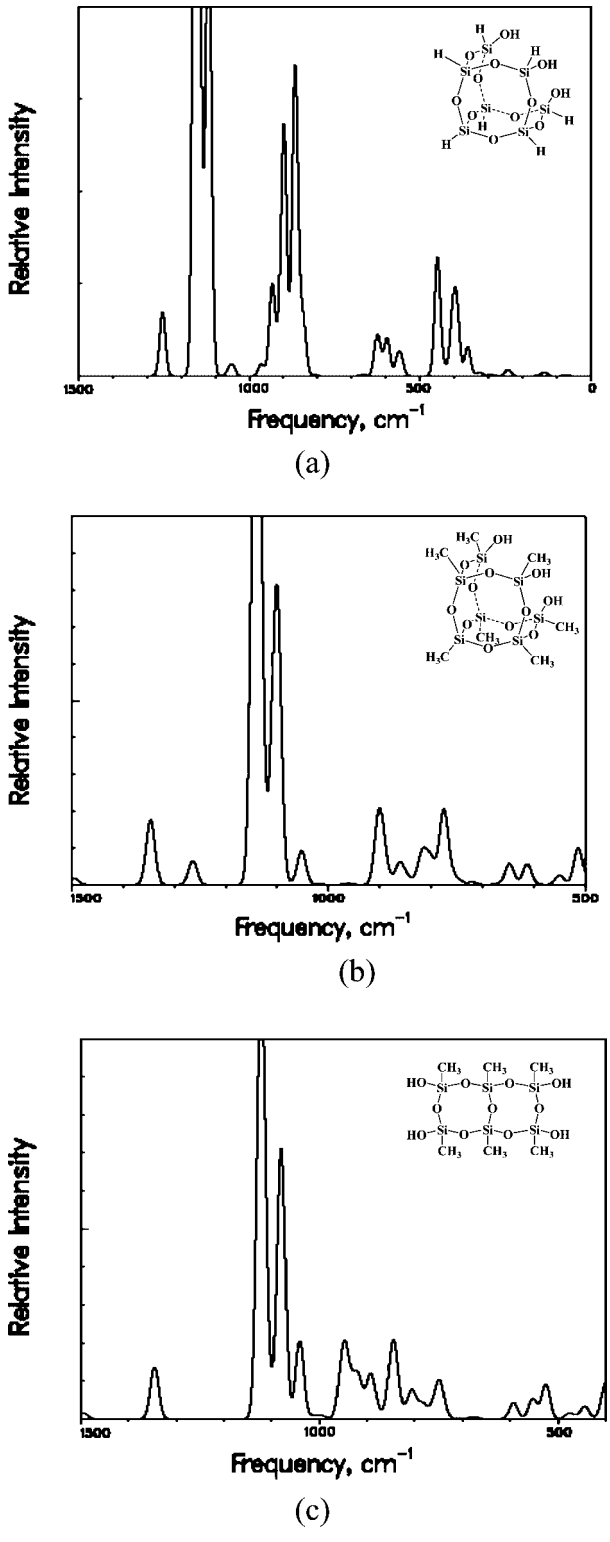

Figure 5. Calculated IR spectra of (a) open T_7 of HSQ ($R_7Si_7O_{12}H_3$ with R = H), (b) open T_7 of MSQ ($R_7Si_7O_{12}H_3$ with R = CH_3), and (c) MSQ Si_6 ladder structure ($R_6Si_6O_7(OH)_4$ with R = CH_3).

Experimental IR spectra for thin PMSQ films cured at various temperatures are presented in Figure 6. The major absorption bands for the initial sample cured at 120 °C match those of the simulated IR spectra, including the Si−CH_3 stretching and wagging bands as well as the $\nu_{\text{ring-asym}}$ and $\nu_{\text{ring-sym}}$ bands (see Table 1). The bands of Si−CH_3 associated with the stretching mode and wagging modes are shown at about 1274 cm^{-1} and at 773 and 825 cm^{-1}, respectively.

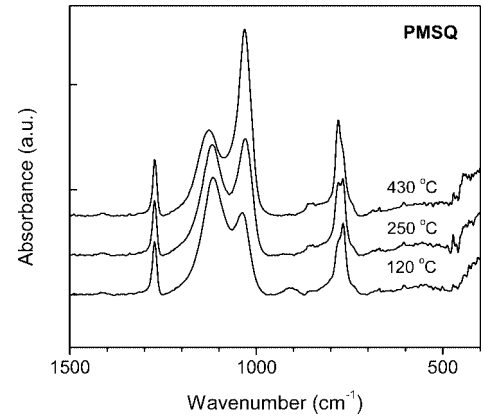

Figure 6. Experimental IR spectra of PMSQ samples cured at various temperatures. The spectra were normalized to keep the same area of the Si−C stretching peak at about 1280 cm^{-1}.

They are in good agreement with the calculated results, although the band positions are not exactly matched. On the basis of the assignment from our theoretical calculation, examination of the IR spectra in Figure 6 shows that the initial PMSQ structure cured at 120 °C is comprised of a more symmetrical structure (cage/open cage), but this is transformed toward a random network structure when cured to the maximum temperature of 430 °C. The initial sample reveals a lower intensity at the $\nu_{\text{ring-sym}}$ absorption band as compared to the intensity of the higher energy $\nu_{\text{ring-asym}}$ band. When cured at 250 °C, the $\nu_{\text{ring-sym}}$ band at 1030 cm^{-1} shows an increase in intensity and the $\nu_{\text{ring-asym}}$ at 1118 cm^{-1} shows a slight decrease in intensity, making the intensities of these two modes comparable. However, upon increasing the curing temperature to 430 °C, the IR spectra of PMSQ show further changes of intensity in the $\nu_{\text{ring-sym}}$ and $\nu_{\text{ring-asym}}$ bands, making the 1030 cm^{-1} band much stronger than the 1118 cm^{-1} band. The increase in intensity of the $\nu_{\text{ring-sym}}$ absorption band indicates that the molecular structure formed in the PMSQ film favors a lower symmetry random network-like structure. At the same time, the weakening of the $\nu_{\text{ring-asym}}$ band gives evidence for the disappearance of the $(Si-O)_4$ ring subunits of the highly symmetrical cage/open cage structures. Therefore, these IR data show (1) the occurrence of solid-state chemical reaction, primarily by secondary condensation of hydroxyl and alkoxy groups, resulting in highly asymmetric Si−O−Si bond structure devoid of $(Si-O)_4$ ring units and (2) volatilization of highly symmetric low molecular weight PMSQ molecules comprising cage/open cage structures,[17] leading to the overall decrease of symmetry toward a random network-like structure.

For comparison with PMSQ, we also investigated the IR spectra of PiBSQ powder (Figure 7) as polymerized and cured at 190 °C and the IR spectra of PPhSQ thin films (Figure 9) as polymerized and cured at 250 and 450 °C, respectively. Even though the IR spectra of various PiBSQ and PPhSQ structures were not calculated here, the microstructures of these materials can be deduced from the IR spectra. The spectrum of PiBSQ at room temperature (Figure 7, curve a) shows, in the frequency range 1000–1200 cm^{-1}, a single strong band at around 1115 cm^{-1} associated with $\nu_{\text{ring-asym}}$ band from the asymmetric Si−O−Si stretch mode

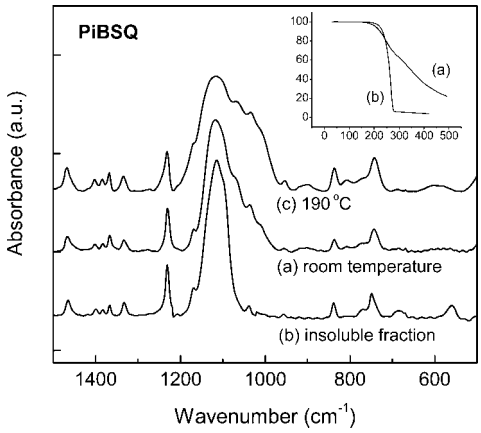

Figure 7. Experimental IR spectra of PiBSQ samples: (a) as-polymerized initial sample, (b) precipitated portion after dissolving the intial PiBSQ in acetone, and (c) initial PiBSQ cured at 190 °C. The inset shows the TGA data of a and b. The spectra were normalized to keep the same area of the Si−C stretching peak at about 1230 cm^{-1}.

of the T_8 cage and a broadened shoulder. This result indicates that the PiBSQ contains a lot of highly symmetric structures, especially in the insoluble fraction of the PiBSQ (Figure 7, curve b) obtained after dissolution in acetone.[30] Indeed, according to the GPLDI-TOF mass spectrum, shown in Figure 8, the insoluble fraction of PiBSQ is comprised of mainly T_8 cage ($R_8Si_8O_{12}$ Na^+: 895.307 *m/z*), open $T_8(OH)_2$ ($R_8Si_8O_{13}H_2$ Na^+: 913.318 *m/z*) cage, and open T_7 cage ($R_7Si_7O_{12}H_3$ Na^+: 813.283 *m/z*) structure species. The TGA data show that the initial PiBSQ sample (Figure 7, inset curve a) lost most of its weight after being heated up to 450 °C, and such weight loss became more dramatic for the insoluble fractionated PiBSQ (Figure 7, inset curve b) which evaporated completely between 200 and 300 °C. As a result, after curing the PiBSQ thin film, the film surface became quite rough. Therefore, the FT-IR measurements of PiBSQ samples (Figure 7) were carried out with powder samples in the KBr pellet. The result for the sample cured at 190 °C shows a significant decrease of the high frequency peak around 1115 cm^{-1}associated with the $\nu_{ring\text{-}asym}$band. In addition, the low-frequency peak at around 1034 cm^{-1} associated with the $\nu_{ring\text{-}sym}$ band is slightly increased. Qualitatively, these results are similar to the PMSQ results and indicate a strong tendency to undergo evaporation of highly symmetric structure species as well as to form random network structures by the secondary condensation reaction during a thermal curing process in the solid state.

As shown in Figure 9, the FT-IR spectrum of the initial PPhSQ sample shows a result similar to that of PiBSQ, namely, the existence of a sharp band at around 1137 cm^{-1} associated with the $\nu_{ring\text{-}asym}$ band and a broad shoulder. As the initial sample is heated to 250 °C, a new peak appears at around 1044 cm^{-1}, which indicates the formation of Si−O−Si bonding involved in low-symmetry structures as a result of the secondary condensation reactions in the solid films. However, unlike PMSQ and PiBSQ, further heating up to 450 °C does not result in the switch in relative intensities between the band at 1137 cm^{-1} and the band at 1044 cm^{-1} accompanied by the decrease of absorption intensity around 1137 cm^{-1} associated with the $\nu_{ring\text{-}asym}$ band. This can be explained by the high thermal stability of the symmetric cage structure species which are contained in the PPhSQ films; indeed, Brown et al. first reported the thermal stability of the PhSQ T_8 cage without evaporation up to approximately 500 °C.[20]

Finally, it is important to point out that our findings on the PSSQ microstructure differ from the conclusions of the previous IR studies.[19,24–27] Previously, Adachi et al.[24] and Xie et al. [25] obtained the IR spectra of PMSQ samples, which are very close to our result from the initial sample (cured to 120 °C), and concluded that they had (double chain) ladder structures, following the earlier conclusion by Brown[19] on PPhSQ samples with similar IR spectra. Such a ladder structure is not favored by our calculated IR results. Moreover, this simple ladder structure is not consistent with the observed chain end concentration[29] nor with the ^{29}Si NMR results of Lee et al.,[26] who showed the presence of various ratios of T_1, T_2, and T_3 structures. The ladder structure is also inconsistent with a careful, detailed measurement of the degree of intramolecular condensation versus average molecular weight from the mass spectrum profile of poly(*n*-propylsilsesquioxane), which exhibits a similar IR pattern, reported by Wallace et al.[33] On the other hand, Lee et al.[26] and Grill and Neumayer[27] analyzed the IR spectra of PMSQ and PMSQ-type OSG samples, respectively, as a simple combination of cage and network structures. Such a simple description of the PSSQ IR spectra, ignoring partially open cage structures, is not realistic enough to provide a meaningful insight into the PSSQ structures and their evolution with process conditions, which are critically needed to understand and improve the functional properties of organosilicate polymers in general.

Conclusion

In summary, we have investigated the solid-state structure of PMSQ and PPhSQ as spin-coated films and PiBSQ as KBr pellet by IR spectroscopy. Quantum chemistry calculations of the IR spectra for model compounds aid in the interpretation of the 1050 cm^{-1} and 1150 cm^{-1} absorption bands associated with the asymmetric Si−O−Si stretching vibrations. The intensity of the lower frequency $\nu_{ring\text{-}sym}$ band, which arises from the Si−O−Si stretch symmetric with respect to the inversion point of the $(Si-O)_n$ ring, is very sensitive to the microstructure as its intensity is very low for highly symmetric cage structures and large for low-symmetry silsesquioxane structures such as branched random networks. The higher frequency $\nu_{ring\text{-}asym}$ band, which arises from multiple Si−O−Si asymmetric stretch vibrations, is stronger when there are $(SiO)_4$ rings that constrain these vibrations to be in phase. The presence of a strong ring-asymmetric stretch band is indicative of highly symmetrical molecular structures, such as the cage and open cage structures. The relative intensity of these two Si−O−Si stretch bands to some degree indicates the density of cage-like versus open network structures in the film. On the basis of such assignments for the Si−O−Si stretching bands, IR spectroscopy offers a simple technique for probing the

(33) Wallace, W. E.; Guttman, C. M.; Antonucci, J. M. *Polymer* **2000**, *41*, 2219.

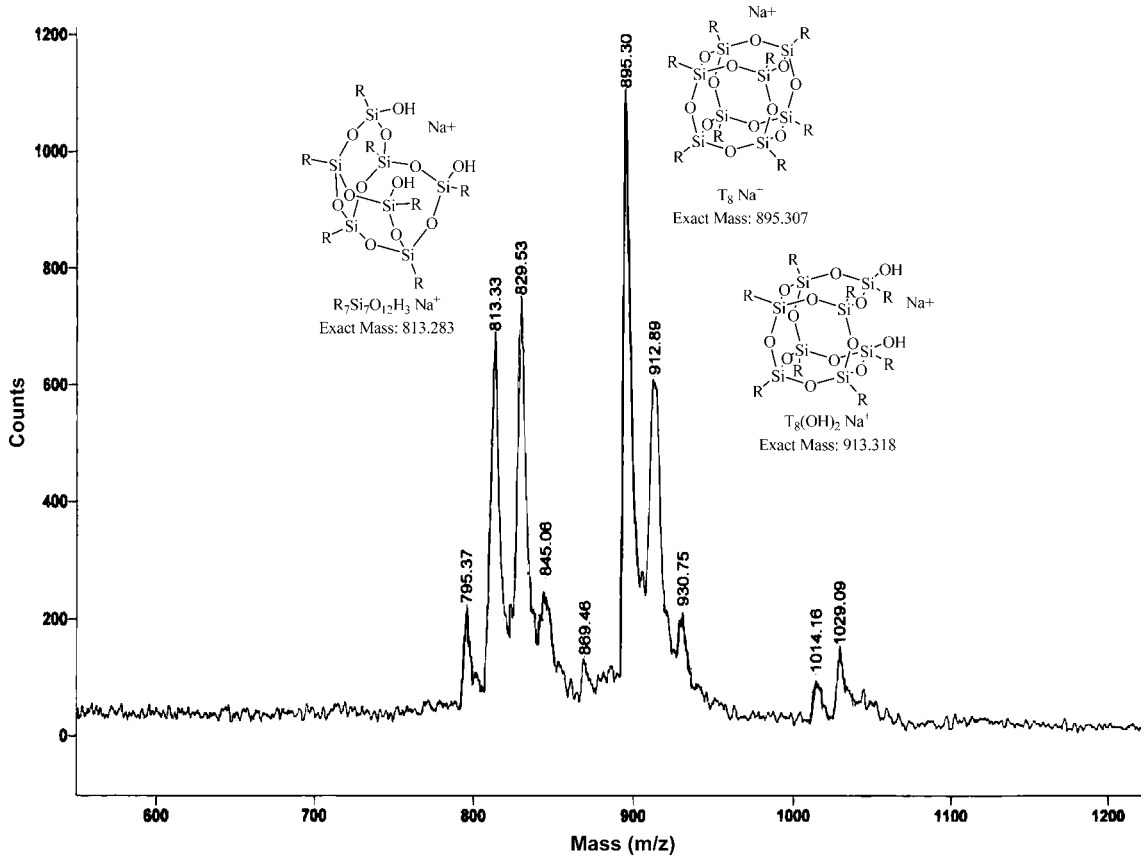

Figure 8. Experimental GPLDI-TOF MS of an insoluble fraction of PiBSQ obtained from initial PiBSQ after dissolving in acetone.

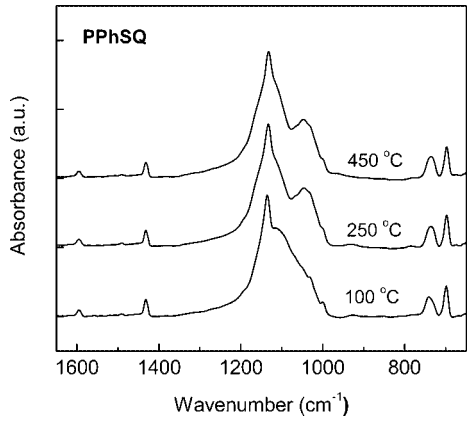

Figure 9. Experimental IR spectra of PPhSQ as a function of curing temperature. The spectra were normalized to keep the same area of the Si−C stretching peak at about 1430 cm^{-1}.

molecular structure of organosilicate polymers and providing insight into the changes of their microstructures during high temperature curing, which can be extended to study OSG films obtained from other preparation methods such as CVD. We demonstrated this method for the thermally cured samples of PMSQ and PPhSQ as spin-coated films and PiBSQ as powders; we found that at high cure temperatures the initially open cage-like structure of PMSQ changes toward a low symmetry, random network structure caused by the secondary condensation and the loss of cage structures via evaporation around 280 °C. Compared with PMSQ, PPhSQ and PiBSQ contain more cage-like structures in the as-polymerized samples; at high cure temperatures, PPhSQ still remains a thermally stable, cage-like structure species while only a small part of PiBSQ remains in the film, primarily as a result of the significantly different evaporation temperatures of the PhSQ cages (ca. 500 °C) and the PiBSQ cage (ca. 280).

Acknowledgment. We thank J. H. Sim and Prof. H.-J. Kim for their help with this work. This work was supported by the "System IC 2010" Project of the Korea Ministry of Science and Technology and the Ministry of Commerce, Industry and Energy and also by the Chemistry and Molecular Engineering Program of The Brain Korea 21 Project.

CM071575Z